Quantum Information and Computation, Vol. 0, No. 0 (2003) 000–000

MAPPING FERMIONS TO QUBITS

OLIVER O'BRIEN
DAMTP, Centre for Mathematical Sciences, University of Cambridge, Cambridge CB30WA, UK
Christ's College, Cambridge, UK

Received (received date)
Revised (revised date)

Your abstract goes here.

Keywords: The contents of the keywords
Communicated by: to be filled by the Editorial

1 Introduction

"Nature isn't classical, dammit, and if you want to make a simulation of nature, you'd better make it quantum mechanical, and by golly it's a wonderful problem, because it doesn't look so easy." - *Dr Richard Feynman* [1]

Ever since Dr Richard Feynman said these famous words at the end of his keynote speech in 1982, one of the main tasks facing quantum computers has been simulating quantum systems. Intuitively a quantum computer should be able to handle this problem better than a classic computer as they operate within the same bizarre world of entanglement and superposition. However, there are many challenges to overcome before quantum advantage can be achieved in this field. We will consider one such challenge in this essay: the optimum mapping scheme from fermions to qubits.

One of the most common classes of quantum systems we wish to simulate are those composed of fermions. In order to simulate these particles we must find a representation for them in terms a quantum computer can process, that is qubits and qubit operators. This poses a fundamental issue as fermions exhibit the non-local property of anti-commutation (**need to explain why it is non-local**), whereas qubits are independent local units. Therefore a non-trival mapping scheme which introduces this non-local behaviour is necessary.

The first such mapping, the **Jordan-Wigner Transformation**, was invented nearly a century ago [2], and we will introduce it in Section 4. More recently, a number of new mappings have been developed including the **Bravyi-Kitaev map** and the **Derby-Klassen map**, which will be discussed in Section 5 and Section 6 respectively. Furthermore, recent research [3] has shown that the **fermionic enumeration** scheme used in a given mapping (we consider solely the Jordan-Wigner case) offers potential for increased locality with no additional

resources. This is elaborated on in Section 7.

It is important to consider how these mappings impact upon the fermionic simulation techniques used. Therefore, in Section 2 we will discuss how VQE and phase estimation can both be used to estimate the ground state energy of a system . Finally, in Section 8 we will compare the relative performance of these mappings in real-world applications (using simulated quantum computers).

2 Applications to fermionic systems

2.1 Estimating ground state energies

Computing the ground state energy of a Hamiltonian is generally the first step in computing the energetic properties of molecules and materials [4]. Chemists have developed classical computational models for estimating the ground state, however, they all rely on approximations. Quantum computing opens up the potential for an exact (*full configuration interaction*) approach, which is unfeasible on a classical computer where it scales exponentially (**verify this is true**) in the number of fermionic modes.

2.1.1 Variational Quantum Eigensolver

A VQE provides an upper bound on the ground state energy of a Hamiltonian by utilising the variational principle:

$$\frac{\langle\psi|\,\hat{H}\,|\psi\rangle}{\langle\psi|\psi\rangle} \geq E_0 \quad \forall\ |\psi\rangle \in \mathcal{H} \tag{1}$$

The algorithm consists of two stages. First a variational ansatz is initialised based on a set of parameters $\boldsymbol{\theta}$. Then, the Hamiltonian is measured a number of times, and the parameters of the ansatz are varied until a minimum is found. This is an example of a variational quantum algorithm, which performs a classical optimisation over a quantum oracle (**is this a correct description**). By exporting lots of the work to a classical computer, VQEs are one of the quantum algorithms that are achievable in the NISQ (Noisy Intermediate-scale Quantum) era.

The preparation of ansatz can be done without any regard for fermions or what underlying wavefunction it represents. Generally a given circuit structure is picked with some of the gates depending upon the parameters (i.e. an $R_z(\theta)$ gate). However, there are some schemes for preparing ansatz that correlate to known wavefunctions, so the wavefunction corresponding to the minimum energy estimate can be found (**check this is true, find example and see if mapping is important** - Unitary Coupled Cluser - gaussian).

It is in the measurement of the Hamiltonian that the mapping becomes important. The Hamiltonian in question will be a combination of fermionic raising and lowering operators, so needs to be mapped to a combination of Pauli operators that can be measured on a quantum computer. **consider measurement strategies that minimise repetitions**. After this mapping has been performed we are left with a qubit Hamiltonian that is a sum of Pauli strings (strings of Pauli operators). Therefore, we can measure the effectiveness of different mappings by the resource costs of implementing this qubit Hamiltonian. We will focus on three metrics (**this bit might be too similar to vqe page 31**):

(i) **Number of qubits:** The less qubits required by the mapping the smaller the quantum computer required to run the simulation.

(ii) **Average Pauli weight:** The average number of Pauli operators in each Pauli string in the Hamiltonian. The smaller the Pauli weight the less gates needed to measure the Hamiltonian, which reduces both the resource cost and the error due to gate infidelity. **Low-weight operators protect against barren plateau** doi:10.1038/s41467-021-21728-w.. **Could potentially elaborate here as it is a bit more complex than just less gates per string it also increases parallelisation and reduces ansatz depth**. **Mention locality**

(iii) **Number of Pauli-strings:** Each Pauli-string is measured separately, so the fewer Pauli-strings to measure, the fewer times the ansatz needs to be initialized and measured.

2.1.2 Quantum Phase estimation

QPE can be used to estimate the energy levels of a Hamiltonian to n bits. This is achieved by applying successive steps of time evolution as a controlled gate with the target being the input state and the control being successive Hadamard ancilla qubits (illustrated in Fig. 1). Then by performing an inverse Quantum Fourier Transform on these ancilla qubits we get a superposition of binary expressions for the energy levels.

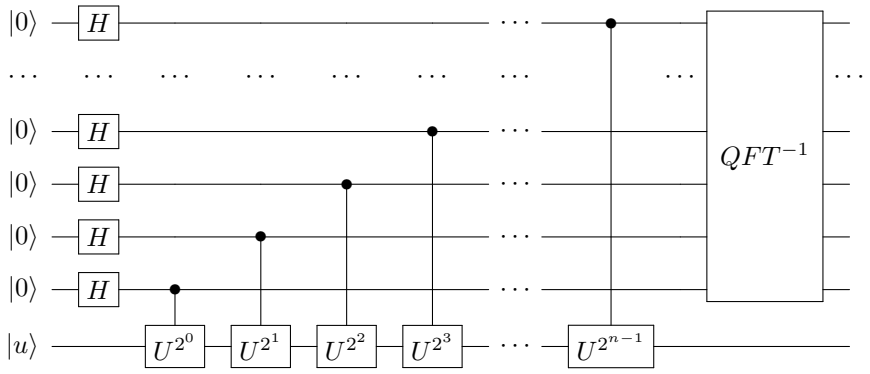

Fig. 1. Circuit diagram of QPE. In order to calcualte energy levels $U = e^{-2\pi i \hat{H}}$ is used.

An important feature of the algorithm is that the guiding state $|u\rangle$ must have overlap with the ground state. This can be seen by working through in detail (we have adapted the following treatment from [5]):

- We can express $|u\rangle$ in the basis of energy eigenstates: $|u\rangle = \sum_i c_i |E_i\rangle$. Therefore, the total state after the application of the Hadamard gates is:

$$\frac{1}{\sqrt{2^n}} \sum_i \sum_x |x\rangle c_i |E_i\rangle \tag{2}$$

- After the application of the controlled gates shown in Fig. 1, this transforms to:

$$\frac{1}{\sqrt{2^n}}\sum_i c_i(|0\rangle + e^{-2\pi i E_i 2^0}|1\rangle)(|0\rangle + e^{-2\pi i E_i 2^1}|1\rangle)\cdots(|0\rangle + e^{-2\pi i E_i 2^{n-1}}|1\rangle)|E_i\rangle \quad (3)$$

  as $x = x_0 2^0 + x_1 2^1 + \cdots + x_{n-1}2^{n-1}$ for $x_i \in \{0,1\}$, this reduces to:

$$\frac{1}{\sqrt{2^n}}\sum_i \sum_x e^{-2\pi i E_i x} c_i |x\rangle |E_i\rangle \quad (4)$$

- By applying an inverse Fourier transform the phase can be extracted:

$$\frac{1}{\sqrt{2^n}}\sum_i \sum_x e^{-2\pi i E_i x} c_i |x\rangle |E_i\rangle \xrightarrow{QFT^{-1}} \sum_i c_i |\text{bin}(E_i)\rangle |E_i\rangle \quad (5)$$

- As E_i is likely not exact to n bits there will be a potential error introduced by the Quantum Fourier Transform, so to be accurate to n bits a few more ancilla qubits will be needed [6].
- By measuring the ancilla bits in the Z basis we will observe E_i to n bits with probability $|c_i|^2$. So to find the ground state energy level, the ground state eigenstate needs to be in the original expansion of the guiding state $|u\rangle$. The larger the amplitude of the ground state eigenstate (c_0) the fewer repetitions of QPE are required before E_0 is measured. Therefore, QPE works better if a guiding state close to the exact ground state is used.

The portion of this algorithm for which fermionic mapping is relevant is the construction of the controlled gates $U^{2^k} = e^{-2\pi i \hat{H} 2^k}$. Not only do the same metrics for the efficiency of the corresponding qubit Hamiltonian listed in Section 2.1 apply, now we need to consider the impact of exponentiation. As the Hamiltonian is the sum of non-commuting Pauli-strings taking the exponential is non-trivial and requires the Trotter-Suzuki approximation [8]. To first order this gives:

$$e^{\frac{-it}{\hbar}\sum_k^m \hat{H}_k} = \left(\prod_k^m e^{\frac{-it\hat{H}_k}{\hbar S}}\right)^S + O(t^2/S) \quad (6)$$

In order to achieve a desired accuracy of ϵ a sufficient number of Trotter steps $S = O(t^2/\epsilon)$ need to be used [5]. The ordering of the terms in this Trotter-Suzuki expansion greatly influences the error and therefore how many Trotter steps are required. This is important to consider as the impact the ordering has varies depending on the mapping chosen as we will discuss in Section 8.

Finally, it is useful to consider how each Trotter step is represented as a circuit. First, we consider that $e^{i(Z_1\otimes Z_2\otimes\ldots\otimes Z_n)\theta}$ applies a phase shift of $e^{i\theta}$ if the parity of the n qubits is even and $e^{-i\theta}$ if the parity is odd. Secondly, it is possible to transform $e^{i(Z_1\otimes Z_2\otimes\ldots\otimes Z_n)\theta}$ into the exponentiation of any Pauli-string by applying R_X or Hadamard gates to change the basis to the X or Y basis, respectively. Therefore, in general the exponential of a n-fold tensor product of Pauli matrices will require $2(n-1)$ CNOT gates centred around one phase-shift gate and enough R_X and Hadamard gates to transform into and out of the necessary basis before and after [7]. The circuit required for computing the term $e^{i(YXZY)\theta}$ is shown in Fig. 2.

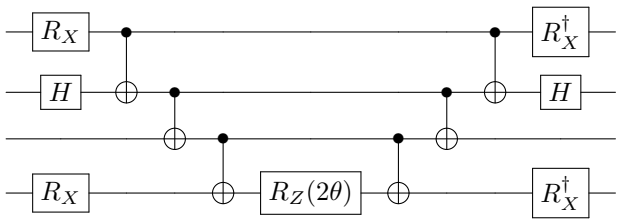

Fig. 2. The circuit required to exponentiate the Pauli-string $YXZY$ by first converting the qubits into the correct basis using R_X and H gates, then computing the parity of the four qubits before applying a single-qubit phase rotation. After this we uncompute the parity and revert to the computational (Z) basis. This is adapted from [7].

2.2 Simulating dynamics - see Nielsen Cheung

3 First and second quantization

From Quantum Field Theory (**citation needed**), we know that fermions must be antisymmetric under exchange. This property is commonly represented in two ways known as the first and second quantization. The first quantization is when the antisymmetry is retained in the wavefunction such as with:

$$|\Phi\rangle = \frac{1}{\sqrt{2}}(|\phi\rangle_1 |\psi\rangle_2 - |\psi\rangle_1 |\phi\rangle_2) \tag{7}$$

This generalises [5] to larger numbers of fermions through a Slater determinant (Eq. 8). This satisfies the antisymmetry condition as swapping any two rows of a determinant produces a sign change:

$$\phi(\boldsymbol{x}_0, ..., \boldsymbol{x}_{N-1}) = \frac{1}{\sqrt{N!}} \begin{vmatrix} \phi_0(\boldsymbol{x}_0) & \cdots & \phi_{M-1}(\boldsymbol{x}_0) \\ \vdots & \ddots & \vdots \\ \phi_0(\boldsymbol{x}_{N-1}) & \cdots & \phi_{M-1}(\boldsymbol{x}_{N-1}) \end{vmatrix} \tag{8}$$

Here M is the number of spin orbitals possible, and N is the number of electrons. Typically we have more spin orbitals than electrons, so the Slater determinant will only contain the N occupied spin orbitals. Acting with fermionic creation and annihilation operators on the first quantization is trivial (if long-winded) as the operators either commute with or act upon each mode.

The second quantisation compresses the information of the Slater determinant by only tracking whether each orbital or fermionic mode is occupied. Therefore the above is written as:

$$\phi(\boldsymbol{x}_0, ..., \boldsymbol{x}_{N-1}) = |f_0, \cdots, f_i, \cdots, f_{M-1}\rangle \tag{9}$$

where f_i (the occupation number) $= 1$ when ϕ_p is occupied, and 0 otherwise. This is termed the Fock basis. Acting on the Fock basis with the fermionic creation and annihilation is more complex and is given by [5]:

$$\begin{aligned} a_p |f_0, \cdots, f_i, \cdots, f_{M-1}\rangle &= \delta_{f_p,1}(-1)^{\sum_{i=0}^{p-1} f_i} |f_0, \cdots, f_p \oplus 1, \cdots, f_{M-1}\rangle \\ a_p^\dagger |f_0, \cdots, f_i, \cdots, f_{M-1}\rangle &= \delta_{f_p,0}(-1)^{\sum_{i=0}^{p-1} f_i} |f_0, \cdots, f_p \oplus 1, \cdots, f_{M-1}\rangle \end{aligned} \tag{10}$$

Therefore, second quantization can be thought of as encoding the antisymmetry of the fermions in the operators rather than the quantum states. All the mappings we will consider are examples of encoding second quantization (**should I consider first quantisation techniques**).

explain advantages of second quantisation vqe chemistry review tranter 2015

4 Jordan-Wigner Transformation

The Jordan-Wigner transformation straight forwardly stores the occupation number of the i-th orbital in the i-th qubit. Therefore, all the non-local behaviour (the parity information) will have to be encoded in the operators [3]:

$$\begin{aligned} a_i &\to \left(\bigotimes_{k=1}^{i-1} Z_k\right) \sigma_i^- \\ a_i^\dagger &\to \left(\bigotimes_{k=1}^{i-1} Z_k\right) \sigma_i^+ \end{aligned} \tag{11}$$

where

$$\begin{aligned} \sigma_i^- &= \frac{1}{2}(X_i + iY_i) = |0\rangle_i \langle 1|_i \\ \sigma_i^+ &= \frac{1}{2}(X_i - iY_i) = |1\rangle_i \langle 0|_i \end{aligned} \tag{12}$$

It is clear to see that these operators act in exactly the same way on a qubit spin basis that the fermionic creation and annihilation operators act upon the Fock basis.

5 Bravyi-Kiteav Map

The Jordan-Wigner transformation uses O(1) qubits to represent each fermionic mode, however it requires O(N) gates to simulate one fermionic operation. This is because it stores the occupation number locally and the parity non-locally. An alternative scheme called the parity basis stores the parity locally and the occupation number non-locally, however this still requires O(N) gates to simulate one fermionic operation [7]. The Bravyi-Kiteav is a halfway house which partially stores both the occupation number and parity non-locally.

The following explanation of the mapping is adapted from [9]. First, we must define a partial order $\preceq$ over a set of binary strings. For $\alpha = \alpha_{l-1} \dots \alpha_0$ and $\beta = \beta_{l-1} \dots \beta_0$, if $\alpha_i = \beta_i$ for $i \geq i_0$ and $\beta_i = 1$ for $i < i_0$, then $\alpha \preceq \beta$. For example:

$$\left.\begin{array}{r} \left.\begin{array}{r} 000 \prec 001 \\ 010 \end{array}\right\} \prec 011 \\ \begin{array}{r} 100 \prec 101 \\ 110 \end{array} \end{array}\right\} \prec 111$$

For the i-th qubit we store the parity of all modes f_k with $k \preceq i$:

$$q_i = \sum_{k \preceq i} f_k \tag{13}$$

The mapping in the eight qubit case is given below (with all sums taken modulo 2) [10]:

$$\begin{bmatrix} 1 & 0 & 0 & 0 & 0 & 0 & 0 & 0 \\ 1 & 1 & 0 & 0 & 0 & 0 & 0 & 0 \\ 0 & 0 & 1 & 0 & 0 & 0 & 0 & 0 \\ 1 & 1 & 1 & 1 & 0 & 0 & 0 & 0 \\ 0 & 0 & 0 & 0 & 1 & 0 & 0 & 0 \\ 0 & 0 & 0 & 0 & 1 & 1 & 0 & 0 \\ 0 & 0 & 0 & 0 & 0 & 0 & 1 & 0 \\ 1 & 1 & 1 & 1 & 1 & 1 & 1 & 1 \end{bmatrix} \begin{bmatrix} f_0 \\ f_1 \\ f_2 \\ f_3 \\ f_4 \\ f_5 \\ f_6 \\ f_7 \\ f_8 \end{bmatrix} = \begin{bmatrix} q_0 \\ q_1 \\ q_2 \\ q_3 \\ q_4 \\ q_5 \\ q_6 \\ q_7 \\ q_8 \end{bmatrix} \tag{14}$$

The maximum number of qubits that rely upon a given mode is $\log_2(N) + 1$ and is attained by f_0 if $N = 2^x$ for some $x \in \mathbb{N}$. Therefore, when we update an occupation number we only need to update $O(\log(N))$ qubits rather than $O(N)$ as in the parity basis.

If we define the set $L(\beta)$ such that $\alpha \in L(\beta)$ if and only if for some i_0, $\beta_{i_0} = 1$, $\alpha_{i_0} = 0$, $\alpha_i = \beta_i$ for $i > i_0$ and $\alpha_i = 1$ for $i < i_0$. Then, in order to find the parity of all the fermionic modes up to a given index i we simply need to find the parity of all qubits in the set $L(i+1)$ [9] (**prove this**). As the set $L(i)$ has at most $\log(i)$ members, we only need to use $O(\log(N))$ gates to compute the parity rather than $O(N)$ gates in the Jordan-Wigner basis. For example, in the eight qubit case the below table gives the parity calculations:

Table 1. Number of tests for WFF triple NA = 5, or NA = 8.

		NP			
		3	4	8	10
NC	3	1200	2000	2500	3000
	5	2000	2200	2700	3400
	8	2500	2700	16000	22000
	10	3000	3400	22000	28000

6 Derby-Klassen Map

7 Fermionic Enumeration

8 Relative performance

9 Introduction

The journal of *Quantum Information and Computation*, for both on-line and in-print editions, will be produced by using the latex files of manuscripts provided by the authors. It is therefore essential that the manuscript be in its final form, and in the format designed for the journal because there will be no futher editing. The authors are strongly encouraged to use Rinton latex template to prepare their manuscript. Or, the authors should please follow the instructions given here if they prefer to use other software. In the latter case, the authors ought to provide a postscript file of their paper for publication.

10 Text

Contributions are to be in English. Authors are encouraged to have their contribution checked for grammar. Abbreviations are allowed but should be spelt out in full when first used.

The text is to be typeset in 10 pt Times Roman, single spaced with baselineskip of 13 pt. Text area (excluding running title) is 5.6 inches across and 8.0 inches deep. Final pagination and insertion of running titles will be done by the editorial. Number each page of the manuscript lightly at the bottom with a blue pencil. Reading copies of the paper can be numbered using any legible means (typewritten or handwritten).

11 Headings

Major headings should be typeset in boldface with the first letter of important words capitalized.

11.1 Sub-headings

Sub-headings should be typeset in boldface italic and capitalize the first letter of the first word only. Section number to be in boldface roman.

11.1.1 Sub-subheadings

Typeset sub-subheadings in medium face italic and capitalize the first letter of the first word only. Section number to be in roman.

11.2 Numbering and Spacing

Sections, sub-sections and sub-subsections are numbered in Arabic. Use double spacing before all section headings, and single spacing after section headings. Flush left all paragraphs that follow after section headings.

11.3 Lists of items

Lists may be laid out with each item marked by a dot:

- item one,
- item two.

Items may also be numbered in lowercase roman numerals:

(i) item one
(ii) item two
    (a) Lists within lists can be numbered with lowercase roman letters,

(b) second item.

12 Equations

Displayed equations should be numbered consecutively in each section, with the number set flush right and enclosed in parentheses.

$$\mu(n,t) = \frac{\sum_{i=1}^{\infty} 1(d_i < t, N(d_i) = n)}{\int_{\sigma=0}^{t} 1(N(\sigma) = n) d\sigma} \,. \tag{15}$$

Equations should be referred to in abbreviated form, e.g. "Eq. (15)" or "(2)". In multiple-line equations, the number should be given on the last line.

Displayed equations are to be centered on the page width. Standard English letters like x are to appear as x (italicized) in the text if they are used as mathematical symbols. Punctuation marks are used at the end of equations as if they appeared directly in the text.

Theorem 1: Theorems, lemmas, etc. are to be numbered consecutively in the paper. Use double spacing before and after theorems, lemmas, etc.

Proof: Proofs should end with □.

13 Illustrations and Photographs

Figures are to be inserted in the text nearest their first reference. The postscript files of figures can be imported by using the commends used in the examples here.

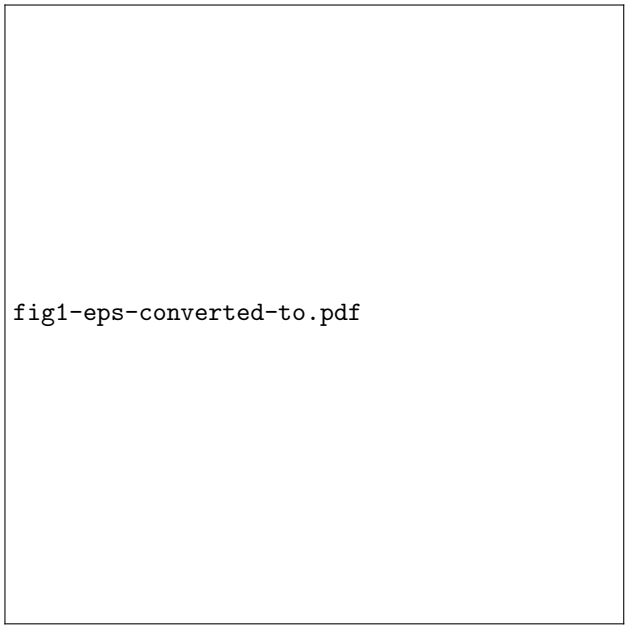

Fig. 3. figure caption goes here.

Figures are to be sequentially numbered in Arabic numerals. The caption must be placed below the figure. Typeset in 8 pt Times Roman with baselineskip of 10 pt. Use double spacing between a caption and the text that follows immediately.

Previously published material must be accompanied by written permission from the author and publisher.

14 Tables

Tables should be inserted in the text as close to the point of reference as possible. Some space should be left above and below the table.

Tables should be numbered sequentially in the text in Arabic numerals. Captions are to be centralized above the tables. Typeset tables and captions in 8 pt Times Roman with baselineskip of 10 pt.

Table 2. Number of tests for WFF triple NA = 5, or NA = 8.

		NP			
		3	4	8	10
NC	3	1200	2000	2500	3000
	5	2000	2200	2700	3400
	8	2500	2700	16000	22000
	10	3000	3400	22000	28000

If tables need to extend over to a second page, the continuation of the table should be preceded by a caption, e.g. "(*Table 2. Continued*)."

15 References Cross-citation

References cross-cited in the text are to be numbered consecutively in Arabic numerals, in the order of first appearance. They are to be typed in brackets such as [11] and [12, 13, 14].

16 Sections Cross-citation

Sections and subsctions can be cross-cited in the text by using the latex command shown here. In Section 16, we discuss ....

17 Footnotes

Footnotes should be numbered sequentially in superscript lowercase Roman letters.[a]

Acknowledgements

We would thank ...

References

References are to be listed in the order cited in the text. For each cited work, include all the authors' names, year of the work, title, place where the work appears. Use the style shown

[a]Footnotes should be typeset in 8 pt Times Roman at the bottom of the page.

in the following examples. For journal names, use the standard abbreviations. Typeset references in 9 pt Times Roman.

pt!

1. Feynman, R.P.. *Simulating physics with computers*. International Journal of Theoretical Physics 1982;21(6-7):467–488. doi:10.1007/bf02650179.
2. Pascual Jordan and Eugene Wigner. *Über das Paulische Äquivalenzverbot*. Zeitschrift fur Physik, 47(9-10):631651, September 1928.
3. Chiew, M. and Strelchuk, S.. *Optimal Fermion-Qubit Mappings*. ArXiv:2110.12792 [Quant-Ph], 25 October 2021. http://arxiv.org/abs/2110.12792
4. Tilly, Jules, Hongxiang Chen, Shuxiang Cao, Dario Picozzi, Kanav Setia, Ying Li, Edward Grant, et al. *The Variational Quantum Eigensolver: A Review of Methods and Best Practices*. ArXiv:2111.05176 [Quant-Ph], 9 November 2021. http://arxiv.org/abs/2111.05176 **look for journal version**
5. McArdle, Sam, Suguru Endo, Alán Aspuru-Guzik, Simon C. Benjamin, and Xiao Yuan. *Quantum Computational Chemistry*. Reviews of Modern Physics 92, no. 1 (30 March 2020): 015003. https://doi.org/10.1103/RevModPhys.92.015003.
6. Nielsen, M.A., Chuang, I.L.. *Quantum Computation and Quantum Information*. Cambridge: Cambridge University Press; 2009. ISBN
7. Seeley, Jacob T., Martin J. Richard, and Peter J. Love. *The Bravyi-Kitaev Transformation for Quantum Computation of Electronic Structure*. The Journal of Chemical Physics 137, no. 22 (14 December 2012): 224109. https://doi.org/10.1063/1.4768229.
   9780511976667. doi:10.1017/cbo9780511976667.
8. Suzuki, Masuo. *Generalized Trotter's Formula and Systematic Approximants of Exponential Operators and Inner Derivations with Applications to Many-Body Problems*. Communications in Mathematical Physics 51, no. 2 (June 1976): 183–90. https://doi.org/10.1007/BF01609348.
9. Bravyi, Sergey, and Alexei Kitaev. *Fermionic Quantum Computation*. Annals of Physics 298, no. 1 (May 2002): 210–26. https://doi.org/10.1006/aphy.2002.6254.
10. Tranter, Andrew, Peter J. Love, Florian Mintert, and Peter V. Coveney. *A Comparison of the Bravyi-Kitaev and Jordan-Wigner Transformations for the Quantum Simulation of Quantum Chemistry*. Journal of Chemical Theory and Computation 14, no. 11 (13 November 2018): 5617–30. https://doi.org/10.1021/acs.jctc.8b00450.
11. P. Horodecki and R. Horodecki (2001), *Distillation and bound entanglement*, Quantum Inf. Comput., Vol.1, pp. 045-075.
12. R. Calderbank and P. Shor (1996), *Good quantum error correcting codes exist*, Phys. Rev. A, 54, pp. 1098-1106.
13. M.A. Nielsen and J. Kempe (2001), *Separable states are more disordered globally than locally*, quant-ph/0105090.
14. A.W. Marshall and I. Olkin (1979), *Inequalities: theory of majorization and its applications*, Academic Press (New York).

Appendix A

Appendices should be used only when absolutely necessary. They should come after the References. If there is more than one appendix, number them alphabetically. Number displayed equations occurring in the Appendix in this way, e.g. (A.1), (A.2), etc.

$$\langle \hat{O} \rangle = \int \psi^*(x) O(x) \psi(x) d^3x \ . \tag{A.1}$$